Clim Dyn
DOI 10.1007/s00382-009-0635-3

# Boreal summer intraseasonal oscillations and seasonal Indian monsoon prediction in DEMETER coupled models

**Susmitha Joseph · A. K. Sahai · B. N. Goswami**

Received: 13 January 2009 / Accepted: 10 July 2009


**Abstract** Even though multi-model prediction systems may have better skill in predicting the interannual variability (IAV) of Indian summer monsoon (ISM), the overall performance of the system is limited by the skill of individual models (single model ensembles). The DEMETER project aimed at seasonal-to-interannual prediction is not an exception to this case. The reasons for the poor skill of the DEMETER individual models in predicting the IAV of monsoon is examined in the context of the influence of external and internal components and the interaction between intraseasonal variability (ISV) and IAV. Recently it has been shown that the ISV influences the IAV through very long breaks (VLBs; breaks with duration of more than 10 days) by generating droughts. Further, all VLBs are associated with an eastward propagating Madden–Julian Oscillation (MJO) in the equatorial region, facilitated by air–sea interaction on intraseasonal timescales. This VLB-drought–MJO relationship is analyzed here in detail in the DEMETER models. Analyses indicate that the VLB-drought relationship is poorly captured by almost all the models. VLBs in observations are generated through air–sea interaction on intraseasonal time scale and the models' inability to simulate VLB-drought relationship is shown to be linked to the models' inability to represent the air–sea interaction on intraseasonal time scale. Identification of this particular deficiency of the models provides a direction for improvement of the model for monsoon prediction.

**Keywords** Indian summer monsoon · Interannual variability · Intraseasonal variability · ENSO · Air–sea interaction

## 1 Introduction

Prediction of monsoon interannual variability (IAV) has been a steaming issue among the meteorological community due to its profound socio-economic impact over the region. Predicting the IAV is of great use to policy makers for agricultural planning, water resource management etc. Monsoon meteorologists have been trying to attain this goal through various statistical and dynamical prediction methods. Attempts to improve the seasonal prediction of Indian summer monsoon rainfall (ISMR) using statistical/empirical techniques have a long history, started by Blanford in the nineteenth century (1884). Since then, many statistical models have been developed and employed (Walker 1923, 1924; Bhalme et al. 1986; Shukla and Mooley 1987; Gowarikar et al. 1989, 1991; Goswami and Srividya 1996; Sahai et al. 2000, 2002, 2003, 2008; Rajeevan et al. 2007). While statistical models offer reasonable skill in predicting ISMR, they fail to predict the extreme monsoons and their skill is limited in providing the ISM evolution in temporal and spatial scales. Hence, dynamical prediction of seasonal rainfall using state-of-the-art general circulation models (GCMs), especially coupled GCMs (CGCMs) provide an alternative over the statistical models (Sperber and Palmer 1996; Kang et al. 2004; Kang and Shukla 2006; Xavier and

**Electronic supplementary material** The online version of this article (doi:10.1007/s00382-009-0635-3) contains supplementary material, which is available to authorized users.

S. Joseph · A. K. Sahai (✉) · B. N. Goswami
Climate and Global Modeling Division,
Indian Institute of Tropical Meteorology, Pune, India
e-mail: sahai@tropmet.res.in

S. Joseph
e-mail: susmitha@tropmet.res.in

B. N. Goswami
e-mail: goswami@tropmet.res.in

Published online: 26 July 2009

Goswami 2007). However, dynamical prediction is limited by the nonlinearity of the monsoon system (Goswami 1998) as well as systematic biases (Gadgil and Sajani 1998) in the current climate models themselves (Kang et al 2004; Wang et al. 2004).

Seasonal prediction of ISM is controlled by relative contributions from externally forced as well as internally generated components (Xavier and Goswami 2007; Joseph et al. 2008). The major contributions from the external forcing are through the ENSO-monsoon teleconnections and the local air–sea interactions over the warm oceans, especially over the eastern equatorial Indian Ocean (EEIO) and Western Pacific (Wang et al. 2005). Indian Ocean Dipole (IOD; Saji et al. 1999; Ashok et al. 2001, 2004; AjayaMohan et al. 2008) and ENSO Modoki (Ashok et al. 2007) are the two other external forcings from the tropical Indo-Pacific basin. While the internal IAV in the atmosphere could be generated largely through non-linear interaction between intraseasonal oscillations (ISOs) and the seasonal cycle (Goswami and Xavier 2005), some contribution could also come from the interactions between the monsoon flow and topography and non-linear scale interactions between high frequency oscillations. Several studies indicate that approximately 50% of the IAV of the seasonal mean of ISM comes from the contribution of the internal component, while the rest coming from the external component (Goswami 1998; Goswami and AjayaMohan 2001; Goswami and Xavier 2005), making it challenging to predict (Kang et al. 2004; Wang et al. 2004; Goswami et al. 2006; Xavier and Goswami 2007). Improved understanding of all these factors is important in order to comprehend the factors limiting the better prediction of ISM using the GCMs.

In the past, several attempts have been made to improve dynamical prediction, but most of them used atmosphere only GCMs (AGCMs; Slingo et al. 1996; Sperber et al. 2001; Kang et al. 2002; Waliser et al. 2003). As a result of seminal role played by coupled processes on IAV of monsoon (Wang et al. 2005), it is imperative that coupled ocean atmosphere models are to be used for seasonal to interannual predictions. This has motivated several international projects like DEMETER (Development of a European Multimodel Ensemble system for seasonal to inTERannual prediction; Palmer et al. 2004), SMIP (Seasonal Prediction Model Intercomparison project), ENSEMBLES etc that uses coupled models for seasonal and longer time scale forecasts.

DEMETER project was intended to develop a multi-model ensemble prediction system and several studies (Kim et al. 2008) show that the multi-model ensemble (MME) prediction system may have better skill over individual models. In this study, we do not rule out this prospect. Instead, we believe that even though the skill of the MME system could be improved using different techniques and schemes, the over-all performance of the system depends basically on the skill of the individual models. With this view, an attempt is made to understand the reasons behind the poor skill of the individual models involved in the DEMETER project, in representing IAV (Fig. 1a). Recently, some studies (Kim et al. 2008; Xavier et al. 2008) using the DEMETER models show that the difficulty of present climate models in predicting the seasonal mean state can be overcome partly by the improvement in the predictability of ISV activity.

It is well documented by several studies that the ISV and IAV of ISM are governed by a common spatial mode of variability (Ferranti et al. 1997; Goswami and AjayaMohan 2001; Goswami and Xavier 2005). The active-break cycles of monsoon are manifestations of monsoon ISOs (MISOs) that arise from the convective coupling in the atmosphere, but modified by air–sea interaction. If the frequency of occurrence of active (break) conditions within a monsoon season is more, it can affect the seasonal mean by making that particular season excess (deficit), thus affecting the IAV (Goswami and AjayaMohan 2001; Goswami 2005; Joseph et al. 2008). Therefore, it is clear that the predictability of seasonal mean is linked with the statistics of ISV. Hoyos and Webster (2007) suggested that in order to reproduce the observed seasonal monsoon rainfall structure, the ISO activity needs to be well simulated in the climate models. Thus, there is a need for the present generation climate models to improve the simulation of ISV and associated air–sea interaction processes in order to predict the observed IAV realistically.

Recent studies (Joseph et al. 2008; Krishnan et al. 2009) demonstrated that drought years are generated by the sustenance of break periods. Joseph et al. (2008) showed from observations that ‘very long breaks’ (VLBs; breaks with duration of more than 10 days) are the fundamental dynamic process responsible for both internally generated as well as forced IAV of ISM; whereas using modeling studies Krishnan et al. (2009) showed that internal feedbacks between monsoon–midlatitude interactions are responsible for producing internally generated droughts, by sustaining breaks. In our observational study (Joseph et al. 2008), we illustrated that 85% of ISM droughts during 1951–2004 are associated with at least one VLB. It was shown that all VLBs are associated with an eastward propagating MJO (Madden–Julian Oscillation; Madden and Julian 1971, 1994), in the equatorial Indian Ocean and air–sea interactions on intraseasonal time scales are responsible for the sustenance of breaks and hence droughts. The remaining 15% droughts may be generated through external agents like ENSO or the nonlinear interactions between different scales over the monsoon region, as mentioned earlier.

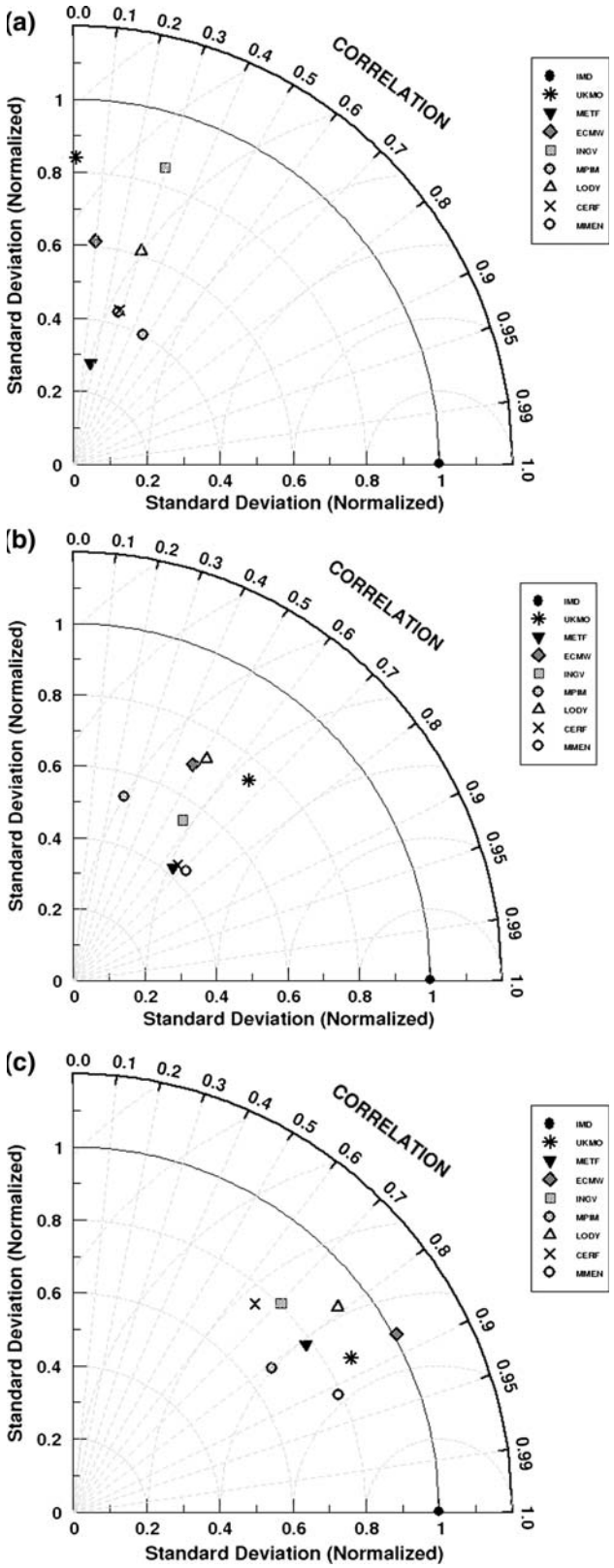


**Fig. 1** (**a**) Interannual variability, (**b**) spatial pattern of climatological seasonal mean and (**c**) mean seasonal cycle, simulated by models and its comparison with observation over IND region

Our objective in this study is to evaluate the skill of the coupled models from DEMETER project in reproducing the relationship between boreal summer (June to September; JJAS) ISV and IAV, with a view to provide insight into the cause of poor skill in predicting IAV. Even though Kim et al. (2008) and Xavier et al. (2008) examined certain aspects of boreal summer ISOs in the coupled model hindcasts from the DEMETER project, none of them addressed the possible cause for the poor relationship between ISV and IAV in detail. To start with, the biases in the DEMETER models in capturing the seasonal mean, mean seasonal cycle, the climatological pattern of seasonal mean and the amplitude and dominant modes of ISV activity are quantified. As mentioned earlier, IAV of ISM and its predictability is very much dependent on several teleconnections around the globe and also the local air–sea interactions over the warm oceans. In this view, we examine how these relationships are incorporated in the models. In the light of the observational study (Joseph et al. 2008), it is tested whether the interaction between IAV and ISV through VLBs is represented in the models. It is analyzed whether the models are able to simulate VLBs properly and whether VLBs in the models are generating droughts? If so, which of the models are better in simulating these features, both spatial pattern and propagation characteristics? How good are the models in simulating the propensity of MJO during droughts? How the air–sea interaction processes associated with VLBs are simulated by the models? It is believed that by addressing these issues, we can get some insight in to the reasons why the models (even if they are coupled) fail to predict the monsoon IAV realistically.

## 2 Datasets used

As mentioned earlier, this study uses the prediction data of seven global fully coupled atmosphere–ocean–land seasonal prediction system from DEMETER project. DEMETER project is oriented to develop a well-validated European coupled multi-model ensemble forecast system for reliable seasonal to interannual prediction (Palmer et al. 2004). The multi-model prediction system has models from the following institutions: CERFACS (European Centre for Research and Advanced Training in Scientific Computation, France), ECMWF (European Centre for Medium-Range Weather Forecasts, U.K.), INGV (Instituto Nazionale de Geofisica e Vulcanologia, Italy), LODYC (Laboratorie d'Oceanographie Dynamique et de Climatologie, France), MetFr (Centre National de Recherches Meteorologiques, France), MPI (Max-Plank Institut für Meterologie, Germany) and UKMO (Met Office, U.K.). Hereafter, the models will be referred as CERF, ECMW, INGV, LODY,

METF, MPIM and UKMO respectively. In order to evaluate the seasonal dependence on skill, the hindcasts were started from 1 February, 1 May, 1 August and 1 November initial conditions, for each model. Each hindcast has been integrated for 6 months and comprises an ensemble of nine members. The data is freely accessible from the website http://data.ecmwf.int/data/d/demeter_daily/all/ maintained by ECMWF, and is available globally at a resolution of 2.5° longitude × 2.5° latitude. Detailed information about the atmosphere and ocean components of all the models is available in Palmer et al. (2004). Here, we have used the hindcasts starting from 1 May, as our focus is to study the boreal summer ISOs. The period of analysis is the JJAS (June to September) season of 1980-2001, which is the common period over which all the models generated hindcasts.

In addition to these, observational datasets used for verification are precipitation pentad data from Global Precipitation Climatology Project (GPCP; Xie et al. 2003), Climate Prediction Centre Merged Analysis of Precipitation (CMAP; Xie and Arkin 1997), gridded daily rainfall data from National Climate Centre (NCC), India Meteorological Department (IMD), Pune (Rajeevan et al. 2006), and SST dataset from ERA-40 reanalysis (same as Reynolds and Smith 1994). GPCP data is obtained at 1° longitude × 1° latitude from the website http://lwf.ncdc.noaa.gov/oa/wmo/wdcamet-ncdc.html for comparing the model hindcasts. The CMAP dataset is obtained at a resolution of 2.5° longitude × 2.5° latitude and it merges satellite and rain gauge data from a number of satellite sources and rain gauge sources. High resolution (1° × 1°) IMD rainfall data for the Indian region is made by analyzing quality controlled daily rainfall data over 1,803 stations distributed over the country. The SST dataset from ERA-40 is a blend of satellite estimates with ship and buoy information. All the observational datasets used here for verification are for the period 1980–2001.

## 3 Results and discussion

Given that DEMETER models are aimed at seasonal to interannual prediction, here we attempt to distinguish the ability of the model in reproducing the seasonal mean. Several studies indicate that the ISV and IAV are governed by common mode of spatial variability (Ferranti et al. 1997; Goswami and AjayaMohan 2001; Goswami and Xavier 2005). In this context, here we examine whether the inability of the models in capturing the seasonal mean arises from their inability in simulating the ISOs reasonably. By examining the ISV in 15 AGCMs, Slingo et al. (1996) showed that the simulation of ISO in the models is closely related to the fidelity in simulating the mean annual cycle (MAC) and basic relationship between sea surface temperature (SST) and precipitation. Hence, it is feasible to examine the model's skill in simulating the MAC and the external components of IAV. Since the dataset is from May to October, here we examine the capacity of the models in simulating the mean seasonal cycle (MSC) instead of MAC.

### 3.1 IAV, seasonal mean and mean seasonal cycle simulation

As mentioned earlier, the simulation of ISV by a model is closely linked to that of the seasonal mean. Hence we first examine the biases of the model in simulating seasonal mean and its variability. The skill of the models in simulating the observed temporal and spatial seasonal mean of the models is assessed here through Taylor diagrams (Taylor 2001). Taylor diagrams can provide a brief statistical outline of how well patterns match each other in terms of their correlation, their root-mean-square difference, and the ratio of their variances (Taylor 2001; Martin et al. 2004). The distance from the origin is the standard deviation (SD) of the field, in this study it is the model, normalized by the standard deviation of the observational climatology. If the standard deviation of the model is same as that of the observation, then the radius is 1. The distance from the reference point to the plotted point gives the root mean square difference (RMSE). Closer the plotted point to the reference point, lesser will be the RMSE. The correlation between the model and the climatology is the cosine of the polar angle (if the correlation between the model and observation is 1, then the point will lie on the horizontal axis). Thus the model which has largest correlation coefficient (CC), smaller RMSE and comparable variance will be close to the reference point (i.e., the observation) is considered to be the best among all.

First, we examine the indices of area averaged seasonal (JJAS) mean rainfall (ensemble mean for 22 years). Figure 1a show the Taylor diagram of the IAV of ISM for IND region (averaged over all Indian land points) averaged seasonal mean rainfall. It is clear from the figure that no model is good in simulating the interannual variation of seasonal mean, in comparison with the observations (IMD data). It is interesting to note that the MME is not capturing the IAV reasonably; it is similar to that of CERF. Considering the variance part, UKMO and INGV are better; but RMSE wise, MPIM is better than the rest. However, the variance of all the models drops drastically when we take the seasonal mean evolution over ISM (65°–100°E; 5°–37.5°N) region (Fig. not shown). Figure 1b indicates that UKMO is better among the models in simulating the spatial pattern of climatological seasonal mean over IND region reasonably well.

Here also, MME behaves similar to METF and CERF. However, over the ISM region (Fig. not shown), INGV and UKMO are realistic in capturing the spatial pattern of climatological seasonal mean in terms of CC, RMSE and ratio of variances. Figure 1c depicts the fidelity of the models in simulating the MSC over IND region. Here, the MME is better over individual models in capturing the MSC. The seasonal cycle of monsoon in MPIM seems to be somewhat peculiar with the precipitation suddenly increasing from May to June, and becoming steady all through the season (June–September) and then decreasing with the beginning of October (Suppl. Fig. S1). The above analysis clearly supports our hypothesis that the performance of the MME system is highly dependent on the skill of individual models included in the MME system.

### 3.2 Intraseasonal activity

In order to understand the amplitude of ISV activity, we have calculated the ISV activity based on Kim et al. (2008). To extract the ISV component, a 20–90 days (since most of the variance in the low frequency mode lies in the band; Kim et al. 2008; Xavier et al. 2008) lanczos filter (Duchon 1979) is applied to each pentad anomaly computed from pentad climatology, for GPCP and the model simulations. For each model, the ISV activity indicates the ensemble mean intensity of ISV, which varies from year to year. Here, we have taken 22 year (1980–2001) data for both the observation and models.

Figure 2 shows the distribution of climatological ISV activity in precipitation from observation and the seven models. The largest amplitude of the observed ISV activity exists around Head Bay of Bengal, west coast of India and near Philippines (Fig. 2a). Among the seven models, UKMO is the best in reproducing these features (Fig. 2h). MPIM has the lowest variance among all the models (Fig. 2g). Similar pattern of climatological ISV activity is exhibited by ECMW and LODY (Fig. 2c, e), which may be attributed to the same atmospheric GCM (IFS) shared by them. An analogous case is observed for CERF and METF also (common AGCM-ARPEGE; Fig. 2b, f). However, CERF and LODY share the same OGCM (OPA8.2), but their simulated structure of the ISV variance is very dissimilar (Fig. 2b, e). Similar is the case with INGV and METF (same OGCM-OPA8.1; Fig. 2d, f). This evidently brings out the dominant role of atmospheric components of DEMETER CGCMs in determining the nature of ISV activity. This has been also pointed out in the recent study by Xavier et al. (2008).

The pattern correlation and root mean square error (RMSE) are calculated between the model-simulated climatological ISV activity and that from observations (GPCP) for each model (Fig. 3a, b respectively). The model with largest pattern correlation and smallest RMSE is closest in simulating the observed ISV activity. The pattern correlation and RMSE is calculated for three regions—the Asian summer monsoon region (ASM; 60°–160°E; 10°S–35°N), the Indian summer monsoon region (ISM; 65°–100°E; 5°–37.5°N) and Indian continent (IND; only land grid points). The three regions (IND, ISM and ASM) are depicted in Suppl. Fig. S2 (IND region is the shaded region, ISM region is the area enclosed by red rectangle and ASM region is the area enclosed by green rectangle). For most of the models, except MPIM, the pattern correlation is more for ISM region than other regions (Fig. 3a). UKMO is the best among the models with leading pattern correlation of 0.78 and 0.73 for ISM and ASM regions respectively. However, its correlation drops to 0.54 for IND region. Over IND region, INGV is the best with a correlation of 0.62. Considering pattern correlation over IND region, INGV is the best and MPIM is the worst. While MPIM has a very weak ISV pattern, its correlation over ASM and ISM regions are reasonably good. This is due to the fact that the grid-to-grid variation of the series is in concurrence with that of GPCP, in spite of the low values. Over all the regions, UKMO has the least RMSE (Fig. 3b). Smallest pattern correlation and largest RMSE is noted for ECMW. ECMW and LODY has comparable pattern correlation and RMSE. In view of pattern correlation and RMSE, UKMO is the best among the models in simulating the characteristics of ISV activity.

### 3.3 Dominant modes of ISV

In terms of space–time characteristics, the boreal summer ISO is characterized by northward and eastward propagating 30–60 day oscillation and the westward propagating quasi-biweekly oscillation. For a CGCM to simulate the IAV realistically, it is desirable that they capture the space–time characteristics of ISOs reasonably well. With this view, we applied wavenumber—frequency spectrum analysis (Wheeler and Kiladis 1999) on the summer precipitation data.

The symmetric component of power of rainfall anomalies reveals the clear presence of 10–20 day and 30–60 day modes in the observation (Figure not shown). Both of these modes are captured reasonably well by METF and CERF; whereas, the signal is almost absent in ECMW, LODY and MPIM (Figure not shown). The quasi-biweekly oscillation with wavenumber 6 has a feeble signal in UKMO and INGV. Figure 4 shows the symmetric component of the power averaged over the wavenumber range 1–4, the wavenumber over which MJO spans. All the models show a peak at around 60 day periodicity in both eastward and westward wavenumbers in comparison with the

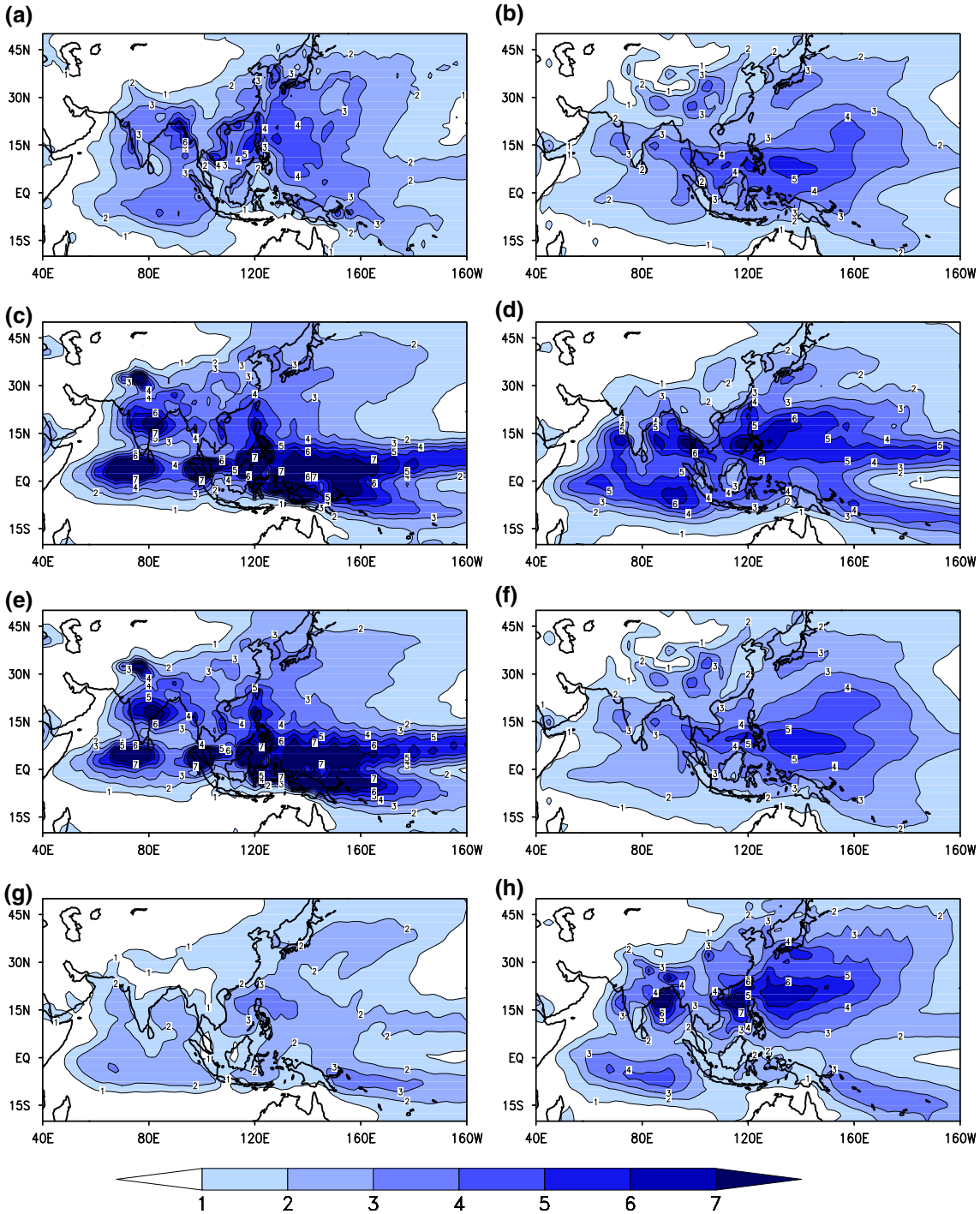


**Fig. 2** Climatological intraseasonal activity of 20–90 day filtered precipitation for **a** GPCP, **b** CERF, **c** ECMW, **d** INGV, **e** LODY, **f** METF, **g** MPIM, and **h** UKMO

observations. The eastward power clearly dominates the westward power in the observations, indicating the presence of MJO. This feature is captured only by CERF and METF. For all other models, the eastward and westward powers are comparable with each other indicating the poor skill of those models in simulating the dominant mode of ISV. This becomes clearer (Suppl. Fig. S3) if we average the power over 30–60 day period range (the period over which MJO spans). Only CERF and METF show a peak at wavenumber 1, as in the observations.

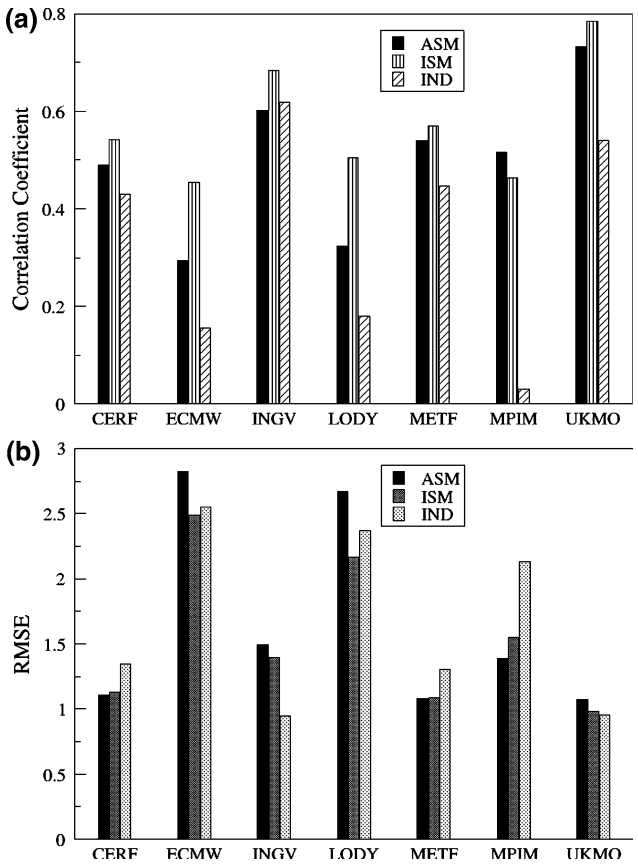


**Fig. 3** (**a**) Pattern correlation and (**b**) RMSE of climatological intraseasonal activity over ASM, ISM and IND regions

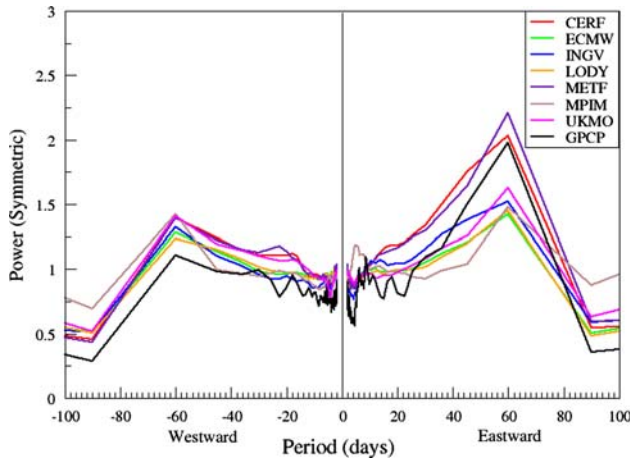


**Fig. 4** Dominant modes of intraseasonal activity of summer monsoon precipitation for GPCP and models

### 3.4 Teleconnection of ISMR with SST

ISMR has several teleconnections around the globe, of which the important ones are those with El-Nino Southern Oscillation (ENSO; Rassmusson and Carpenter 1983), North Atlantic Oscillation (NAO; Rajeevan et al. 1998), North Pacific Oscillation (NPO; Walker and Bliss 1932), Eurasian snow cover (Bamzai and Shukla 1999) and Indian Ocean Dipole (IOD; Saji et al 1999). The relationship of ISMR with the above-mentioned factors are well known and plenty of research has been done in the past and also going on in the present. As mentioned earlier, IAV of monsoon and hence its predictability is very much dependent on such teleconnections. Therefore, in this section, we estimate the concurrent correlation of ISMR with global SST (Fig. 5). Negative correlations of the order of −0.4 are noted in the equatorial central Pacific and Bay of Bengal (BoB) region in the observations. Positive correlations of the order of +0.4 are observed in the north Pacific Ocean. The negative correlation over the equatorial Pacific is captured by all the models and most of them overestimate the relationship. This strong reliance of the model ISMR on the SST over equatorial central Pacific indicates that the IAV of the models are mainly controlled by external forcing. In INGV, the correlation over Nino3 region is about −0.8. This shows that IAV of INGV is very much dependent on ENSO forcing. Another interesting feature is that almost all models failed to capture the negative correlations over BoB. Most of the models reproduced the positive correlations over the north Pacific. It is interesting to note that the models with same AGCM show disparate pattern. The skill of the models in simulating the teleconnection pattern is summarized in a Taylor diagram (Fig. 5i), which illustrates that all models failed to capture the relationship and have large variance (almost double) compared to observations.

### 3.5 Local SST–rainfall relationship

Local air–sea interactions over the warm waters has an important role in the IAV of Indian monsoon rainfall (Kang and Shukla 2006; Wang et al. 2005). While over most parts of the world, rainfall and SST are positively correlated, over the warm waters of eastern Indian Ocean and Western Pacific, the correlation is low and over some parts negative. This may be attributed to the fact that above a threshold value of SST (about 28°C), SST and rainfall are poorly correlated (Gadgil et al. 1984) and generally over the warm waters of Indo-Pacific region, the SST is above this threshold value. The ability of DEMETER models in capturing the observed local air–sea interaction is examined in this section.

Figure 6 shows the correlation coefficients (significant at 5% level) for both observations and models. The observed SST–rainfall relationship is positive over the western and eastern parts of south Indian Ocean; whereas it is negative over western and northwestern Pacific Ocean (Fig. 6a). In the models, the SST–rainfall relationship is

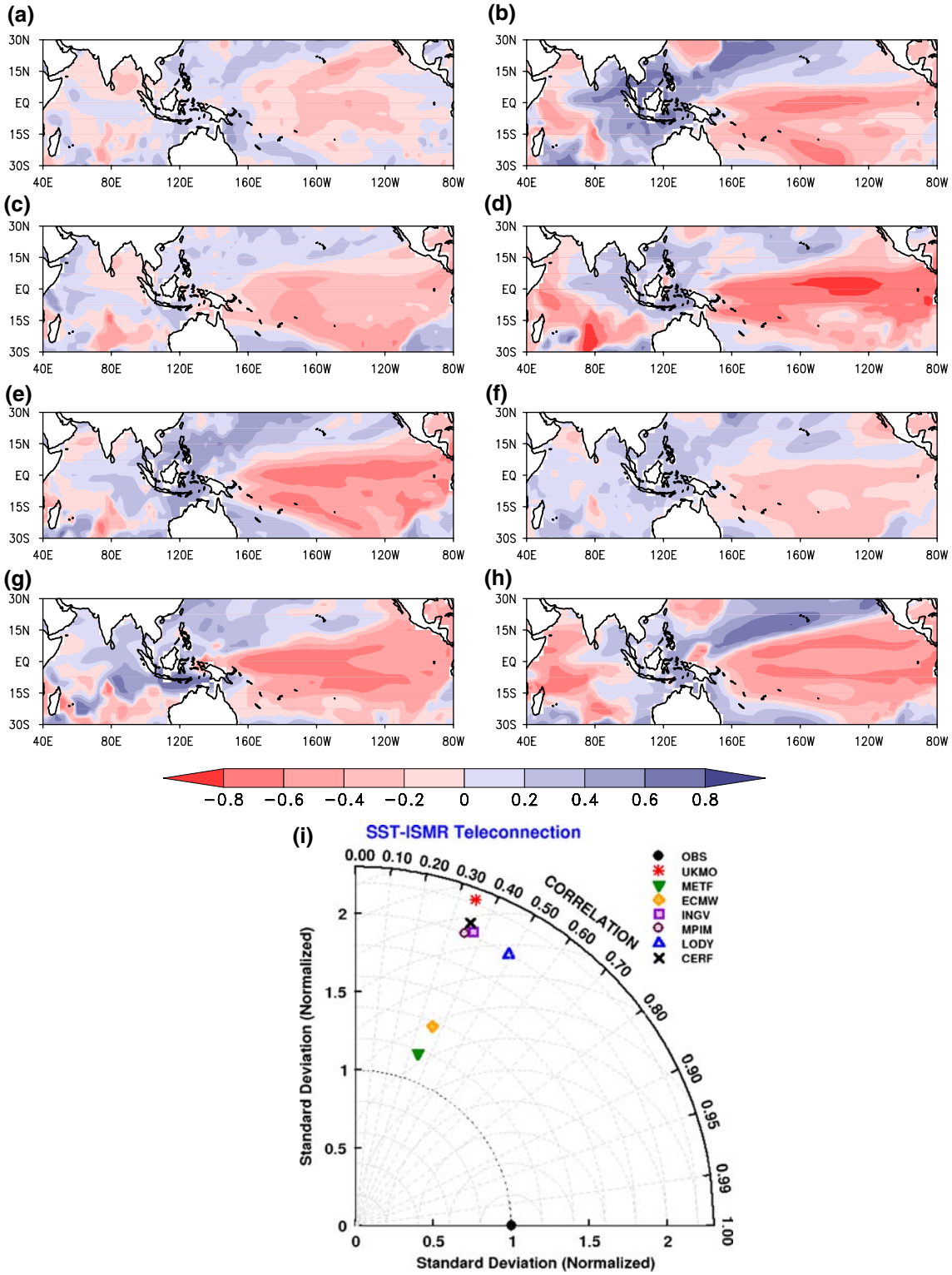


**Fig. 5** Concurrent teleconnection pattern between ISM rainfall and JJAS SST for observation and models. **a** OBS, **b** CERF, **c** ECMW, **d** INGV, **e** LODY, **f** METF, **g** MPIM, **h** UKMO

significantly positive over most of the oceans. The relationship is identical for the models sharing the same AGCM (ECMW and LODY; METF and CERF), which is indicative of the dominant role of atmospheric component over the oceanic one in determining the relationship. Most of the models failed to capture the non-linear relationship

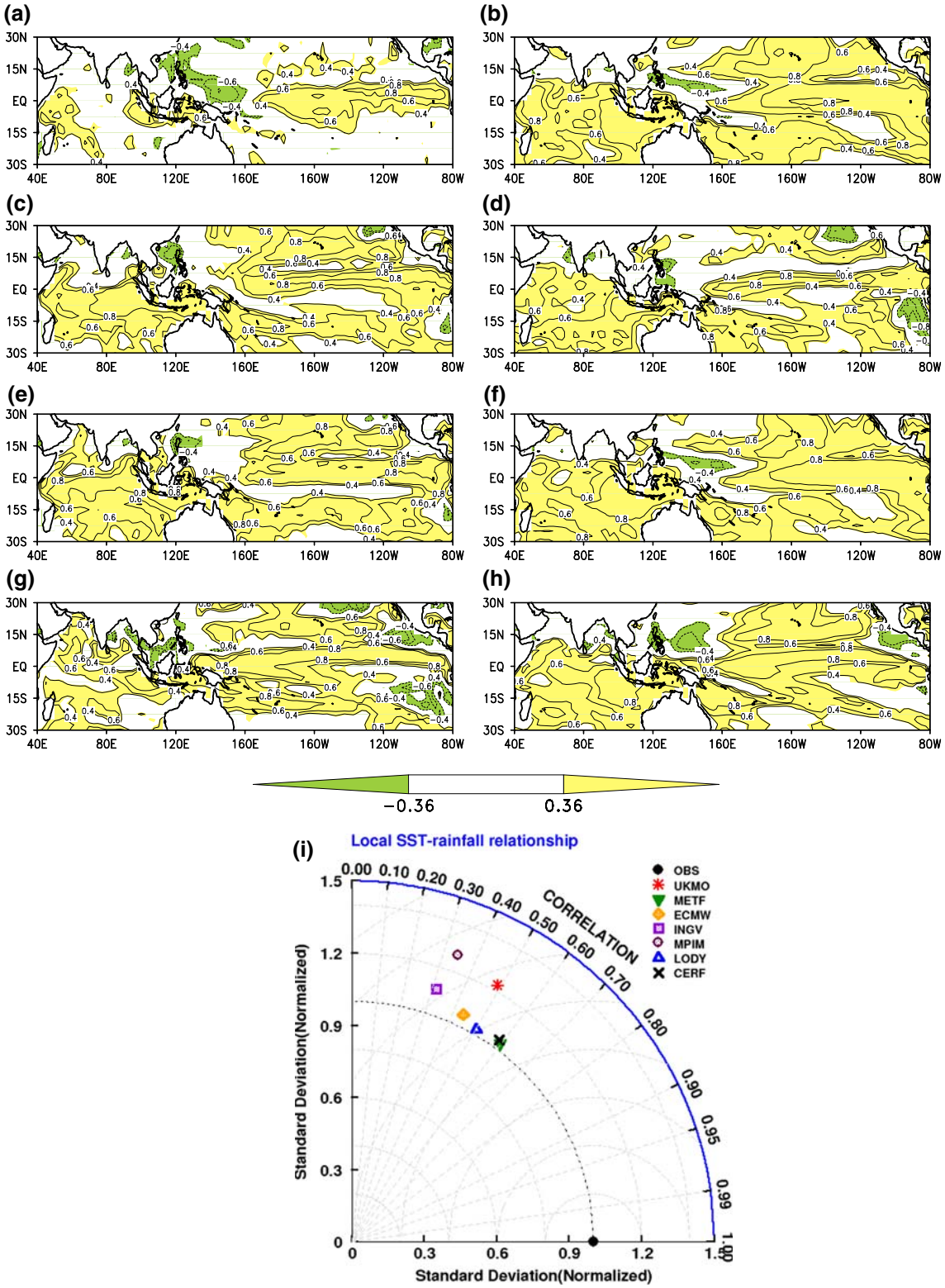


**Fig. 6** Local SST–rainfall relationship for observations and models at 5% significance level. **a** OBS, **b** CERF, **c** ECMW, **d** INGV, **e** LODY, **f** METF, **g** MPIM, **h** UKMO

between the SST and rainfall with the threshold value over the warm pool region. The results noticed in Fig. 6a–h are summarized in the Taylor diagram (Fig. 6i). It is clear from Fig. 6i that all models failed to replicate the observed local SST–rainfall relationship in all aspects (correlation, RMSE and ratio of variances).

### 3.6 Interactions between IAV and ISV through VLBs

Both Joseph et al. (2008) and Krishnan et al. (2009) demonstrated that VLBs are the common seminal factor for producing droughts. While Joseph et al. (2008) showed that VLBs could be generated by air–sea interaction on intraseasonal time scales; Krishnan et al. (2009) suggested that they can also be produced by tropical–midlatitude interactions. In this study, we have tested only the hypothesis by Joseph et al. (2008). It was shown by Joseph et al. (2008) that during VLB, there exists an eastward propagating MJO in the equatorial Indian Ocean, which may give rise to a divergent field north of the equator. This divergent field may generate Rossby type of wave that moves northwestward towards the Indian region, leading to the sustenance of breaks. Wavenumber–frequency spectrum analysis also confirmed that MJO is dominant in the equatorial region during drought years, similar to the ones observed during winter season over the region. The study also indicated that air–sea interaction on intraseasonal time scale is necessary and sufficient to cause VLB and ISM droughts. This hypothesis for the origin of droughts is tested here in the DEMETER models in detail. This particular study also attempts to investigate why the models are able/unable to capture the VLB-drought relationship.

#### *3.6.1 Association between VLBs and droughts in ISM*

Following the criterion used in Joseph et al. (2008), we have identified VLBs from IMD rainfall data and models. We identified break spells when the standardized precipitation anomalies averaged over central India (73°–82°E; 18°–28°N; CI region) is less than 1.0 for consecutive 4 days. If the break spells have duration of more than 10 days, they are identified as VLBs. The total number of VLB spells identified by the models over the 198 year period (22 years × 9 members) are as follows: CERF-5; ECMW-38; INGV-25; LODY-39; METF–3 and UKMO-54. Surprisingly, no VLBs were identified by MPIM. In all the models, majority of the break spells are found in the typical monsoon months of July and August, in concurrence with the observations. The total number of drought years simulated by each model and the drought years that co-occurred with VLBs are given in Fig. 7. In the observational study (Joseph et al. 2008), we have shown that 85% of monsoon droughts (13 ISM droughts emerged during the 57 year period 1951–2007) are associated with VLBs. None of the models reproduced this relationship. The total number of drought years produced by INGV and UKMO over the 198 year period is comparable with that of the observations. In the case of CERF, only 14% of drought years emerged with VLBs; whereas it is 32% for ECMW, 35% for INGV, 36% for LODY, 6.25% for METF, 0% for MPIM and 40.5% for UKMO. This clearly indicates that all models failed to replicate the VLB-drought relationship noted in the observations. The absence of VLBs and minimum number of drought years in MPIM is attributed to the low IAV of the model. For the model, out of the 198 years, 192 are normal years and 6 are drought years. MPIM also has low ISV.

As this section brings out the deficiency of models in reproducing the VLB-drought relationship, the following question arises. Why VLBs in the models fail to produce droughts? Whether the processes responsible for causing the interaction between IAV and ISV through VLBs are not properly incorporated in the DEMETER models? Hence, a detailed analysis is done, following Joseph et al. (2008) to answer these questions.

#### *3.6.2 Spatial distribution of VLB anomalies*

In order to distinguish how well the models capture the association of regional anomalies with global features, we composited the precipitation anomalies during VLBs, for observations and for each model. Since IMD rainfall data is available only over Indian land, we have used CMAP data for comparing the spatial characteristics with the models. None of the models reproduced the features apparent in observations (Fig. 8). Since no VLB was identified by MPIM, here we have only six models for comparison. The "quadruplet" structure (Krishnan et al. 2000; Annamalai and Slingo 2001) with the presence of negative rainfall anomalies over Indian region and maritime continents and positive anomalies over equatorial Indian Ocean and over northwest Pacific, is absent in most of the models. The tilting of the suppressed rainfall anomalies from the maritime continents towards Indian region indicates the Rossby wave dynamics (Fig. 8a; Krishnan et al. 2000; Joseph et al. 2008). Most of the models, except UKMO (Fig. 8g) detained this feature to some extent. Only CERF and

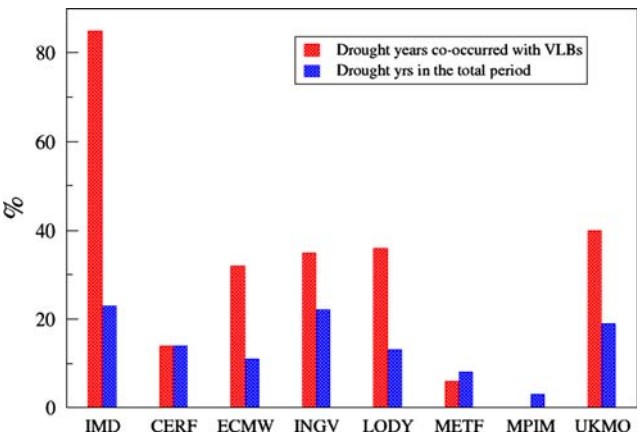


**Fig. 7** VLB-drought relationship in the observation and models

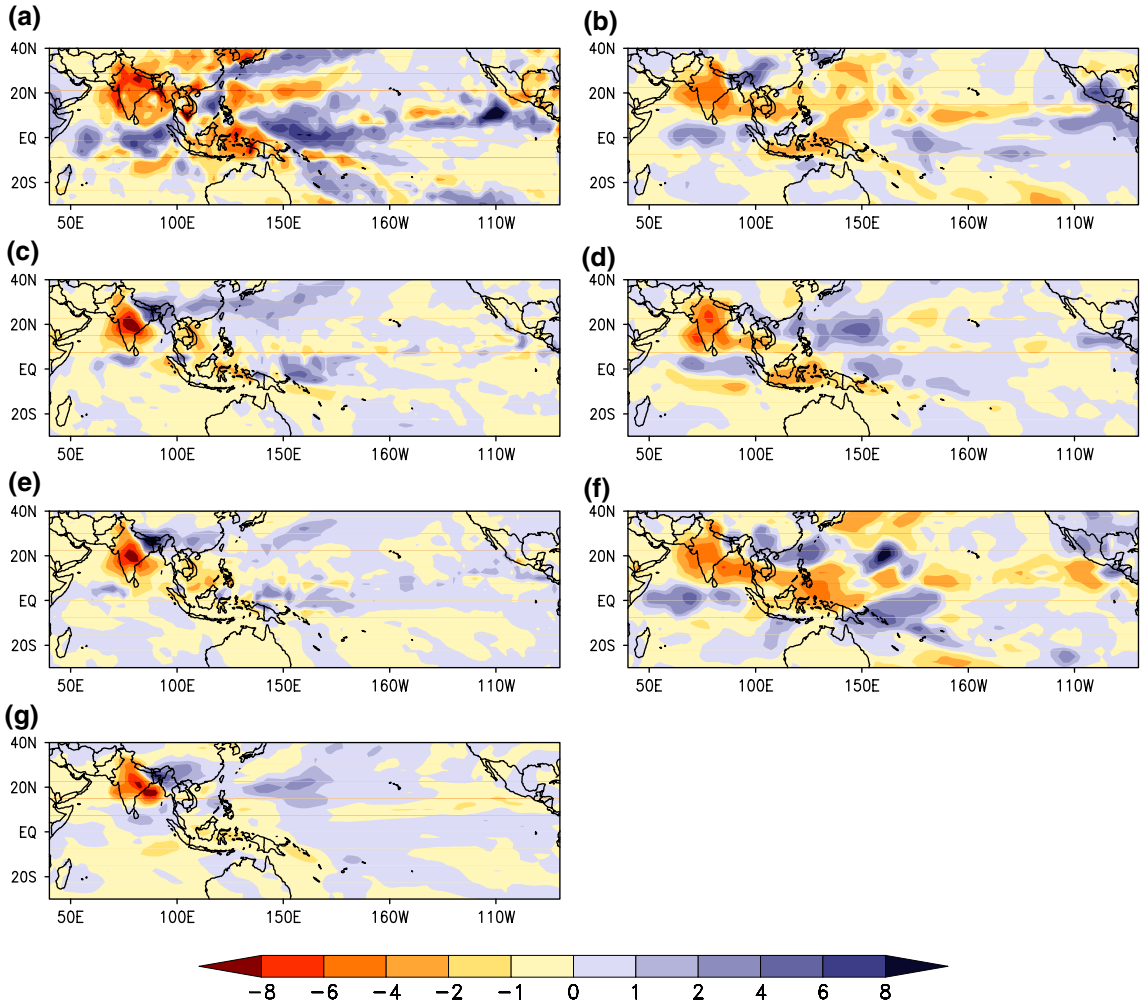


**Fig. 8** Composite rainfall anomalies in mm/day during VLBs in observation and models. **a** CMAP, **b** CERF, **c** ECMW, **d** INGV, **e** LODY, **f** METF, **g** UKMO

METF (Fig. 8b, f) captured the suppressed convection in the west Pacific reasonably. The strong negative anomalies noticed all along the equatorial Pacific in the observation are not clear in any of the models. In METF and UKMO, positive anomalies prevail over the region, which indicate their poor Pacific response.

### *3.6.3 Propagation of rainfall VLB anomalies*

Joseph et al. (2008) indicated that during VLBs, there exist an eastward propagating MJO in the equatorial Indian Ocean; and well organized northward movement of suppressed convection anomalies along the Indian longitudes. Since, we are concerned about the ISO signal, we have filtered the rainfall anomalies during VLBs over 20–90 day band using lanczos filter (Duchon 1979). The eastward (averaged between 5°S and 5°N; Figure not shown) and northward (averaged between 70° and 90°E; Fig. 9a) propagating ISOs are evident in CMAP VLB anomalies. Figure 9b–g depicts the VLB anomalies averaged over Indian longitudes, for the models. None of the models, except METF show clear eastward movement; INGV also exhibit a feeble eastward signal (Figure not shown). Surprisingly, all models failed to capture the northward movement.

Failure of the models in capturing the northward propagation prompted us to investigate the reason behind it. It was shown by Jiang et al. (2004) that the vertical easterly shear is important for northward propagation of the convection band in the northern Hemisphere. They indicated that the vertical easterly shear couples the baroclinic and barotropic modes in the free atmosphere and leads to the generation of barotropic vorticity and anomalous low level convergence to the north of the convection. This further leads to the northward shift of the moisture convergence in the boundary layer and thus ISO convection. Hence, failure of the models in capturing the northward movement of VLB anomalies may be related to the vertical easterly shear (200 hPa wind minus 850 hPa wind). It may be noted from Fig. 10a that easterly shear of more than 20 m $s^{-1}$ is

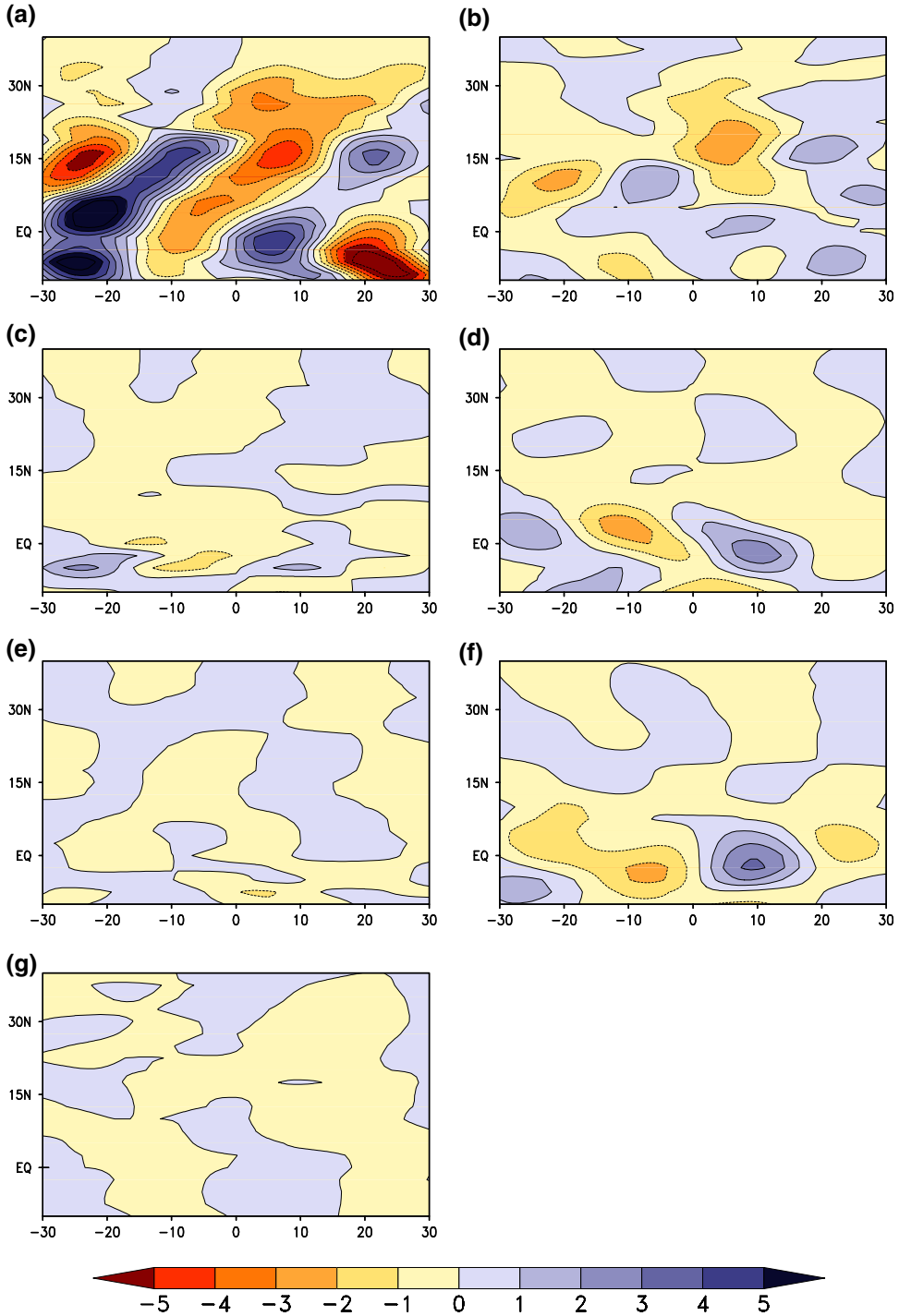


**Fig. 9** Propagation characteristics of rainfall anomalies in mm/day during VLBs averaged over 70°–90°E. Here, zeroth day is the starting day of VLBs. **a** CMAP, **b** CERF, **c** ECMW, **d** INGV, **e** LODY, **f** METF, **g** UKMO

required over a large region (5°–20°N; 40°–120°E). The vertical shear simulated by all the models is too weak (Fig. 10), indicating why models failed to replicate the northward movement of VLB anomalies.

### *3.6.4 Propensity of MJO during drought years*

It was shown by Joseph et al. (2008) that summers of drought years are like winter season with higher propensity of MJO in the equatorial region. Therefore, here we carried out wavenumber—frequency spectrum analysis (Wheeler and Kiladis 1999) over the latitudinal band 15°S–15°N for the drought years identified by each model. The only model that detained MJO during drought years is METF (Figure not shown). Since MJO occurs in the wavenumber range 1–4 and within the period range of 30–60 days, we averaged the power in the symmetric component of rainfall spectra to confirm whether the signal captured by the models is

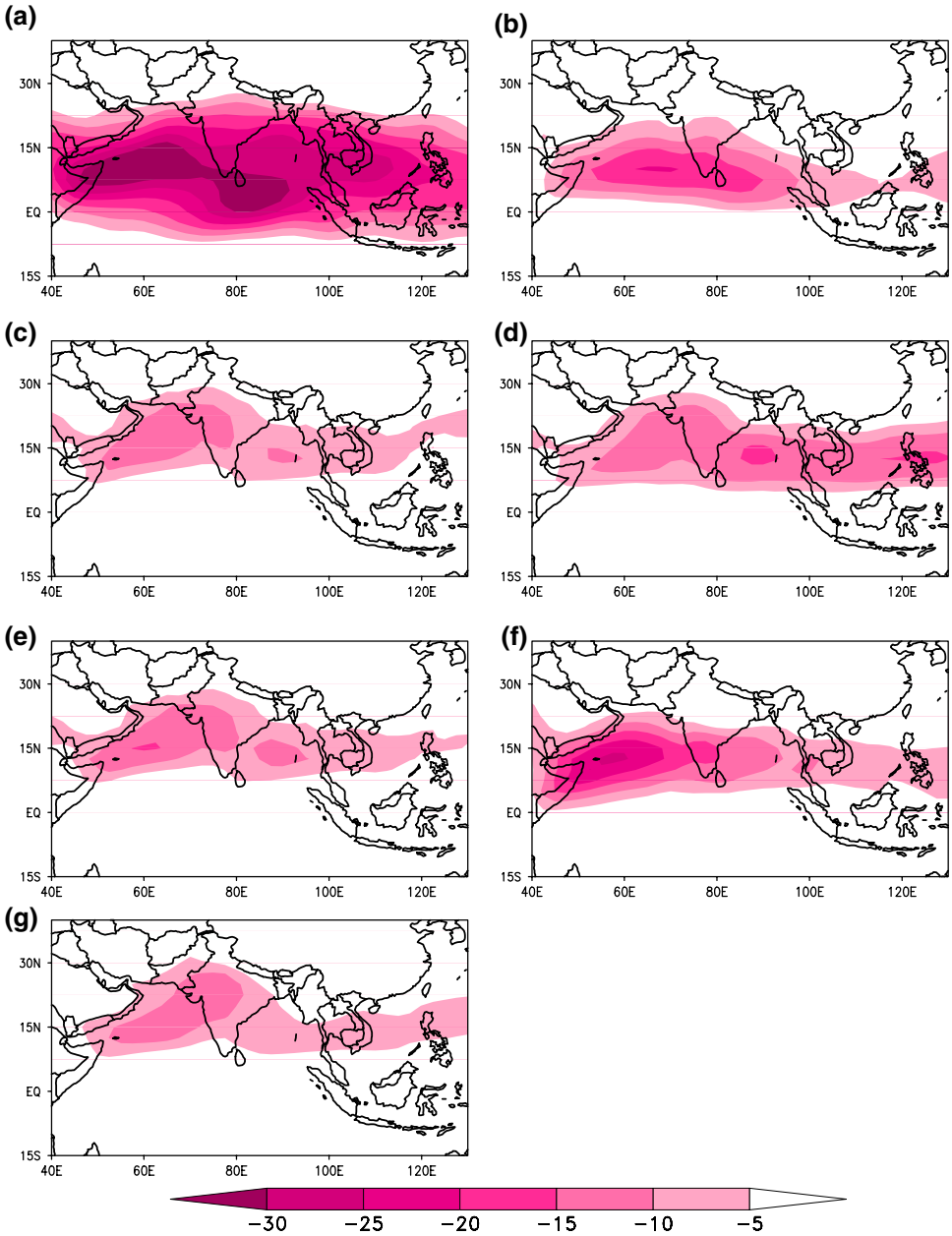


**Fig. 10** Vertical easterly shear (200 hPa wind minus 850 hPa wind) in m/s during VLBs. **a** NCEP, **b** CERF, **c** ECMW, **d** INGV, **e** LODY, **f** METF, **g** UKMO

MJO or not. It is obvious from the analysis that the signal captured by METF is MJO only and all other models failed to capture this feature (Fig. 11). Although some models (ECMW and INGV) show some dominant eastward power over westward power in the wavenumber range 1–4 (Fig. 11a), they failed to simulate the highly dominant eastward power in wavenumber 1, over 30–60 day period range (Fig. 11b).

### *3.6.5 Air–sea interaction during VLBs*

It was demonstrated by Joseph et al. (2008) that during VLBs, the western Pacific warm pool is extended to the central and eastern Pacific and warm SST anomalies prevail over equatorial central Pacific. They showed that these warm SST anomalies generate atmospheric responses in both intraseasonal and interannual time scales; leads to the eastward propagation of MJO, which in turn leads to VLBs and hence droughts. They also noticed that westerly wind anomalies (westerly wind events; WWEs) persevering for about 10–15 days during VLBs are responsible for the extension of the warm pool to the east. Thus, air–sea interaction on intraseasonal time scale is imperative for the generation of VLBs. In this section, we investigate whether the model's inability to simulate the VLB-drought relationship is linked to their ability/inability to simulate the

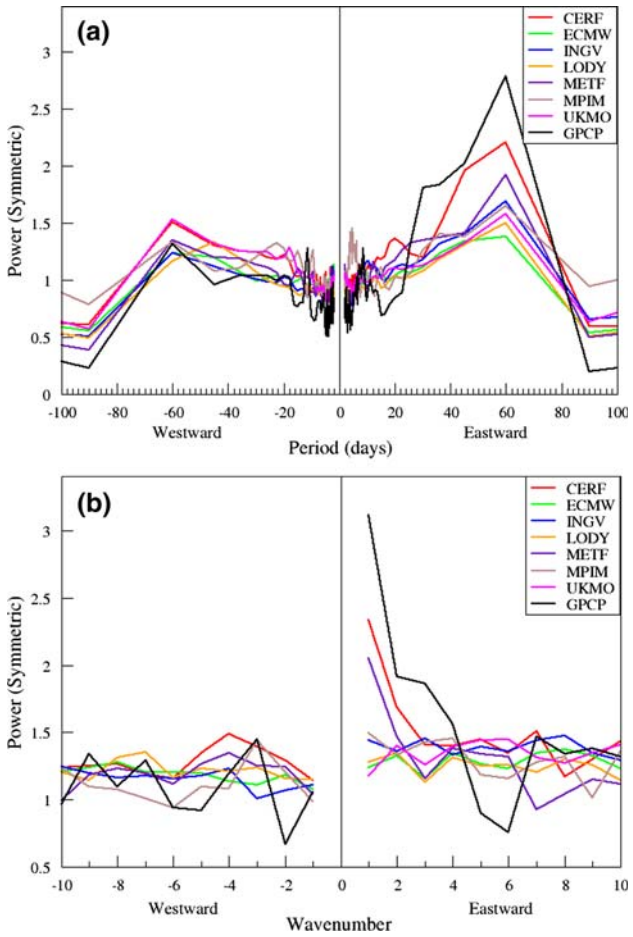


**Fig. 11** Propensity of MJO during drought years in GPCP and models. Power of the symmetric component of rainfall averaged over (**a**) wavenumber range 1–4 and (**b**) period range of 30–60 days

air–sea interaction on intraseasonal time scale. It is clear from Fig. 12a, b that most of the models failed to capture these air–sea interactions reasonably. Even though some models produce westerly wind anomalies during VLBs, they are not associated with the extension of warm pool. The extension of warm pool is exhibited only by CERF, that too to a small extent (Fig. 12b). This reveals the fact that air–sea interaction on intraseasonal time scale is not well represented in the DEMETER models. This is consistent with the finding in Sect. 3.2 where we showed that the ISO characteristics in the DEMETER coupled models are primarily driven by the atmospheric component.

## 4 Summary and conclusions

In this particular study, a detailed investigation has been carried out to understand the reasons behind the poor skill of seven atmosphere–ocean coupled models from DEMETER project in simulating the IAV and its interactions with ISV during boreal summer. It is illustrated that the poor skill of individual models can considerably affect the overall performance of DEMETER MME system. Since, the predictability of ISM rainfall is closely linked to relative contributions from internally and externally generated components of IAV (Xavier and Goswami 2007; Joseph et al. 2008), the contributions from the external component as well as internally generated component are analyzed to unravel the difficulty of the models in reproducing and predicting the observed IAV and its interactions with ISV.

Analyses indicate that while UKMO reproduce the intraseasonal variance, mean seasonal cycle, and the climatological pattern of seasonal mean rainfall reasonably well, it has severe problems in simulating the dominant modes of ISV, SST-ISMR teleconnection pattern and the observed air–sea interaction. On the other hand, CERF which has reasonable teleconnection pattern and air–sea interaction pattern and which simulates the dominant modes of ISV realistically, has problems in capturing the seasonal cycle and IAV. The simulations are not good for MPIM, because of its weak variability in both interannual and intraseasonal time scales. Most of the models, particularly INGV, overestimate the ENSO–monsoon relationship. This indicates that in these models, contribution from external component, predominantly the ENSO–monsoon teleconnection, may be overriding the contributions from internal one.

The VLB-drought relationship, indicating the association of most of the ISM drought years with VLBs as identified in the observational study of Joseph et al. (2008), is poor in most of the DEMETER models. While, INGV and UKMO have more number of drought years, none of the models is able to simulate the observed VLB-drought relationship. The absence of VLBs and minimum number of extreme monsoon seasons in MPIM is indicative of the model's weak ISV as well as IAV representation. Failure of the models in reproducing the northward propagation of VLB rainfall anomalies is attributed to the weak vertical easterly shear (200 hPa wind minus 850 hPa wind). It is clear from the analyses that air–sea interaction on intraseasonal time scales observed during VLBs is not well represented in the DEMETER models. This points out that even though some models produce VLBs, they may not be generated due to air–sea interaction on intraseasonal time scales. They may be generated through monsoon-midlatitude interactions, as suggested by Krishnan et al. (2009) or through nonlinear scale interactions over the monsoon regions. However, the analysis of these aspects is beyond the scope of the present study.

The present study provides some evidences that in order to simulate the observed IAV realistically, the contributions from both the external and internal components are to be incorporated properly. In the DEMETER models, the

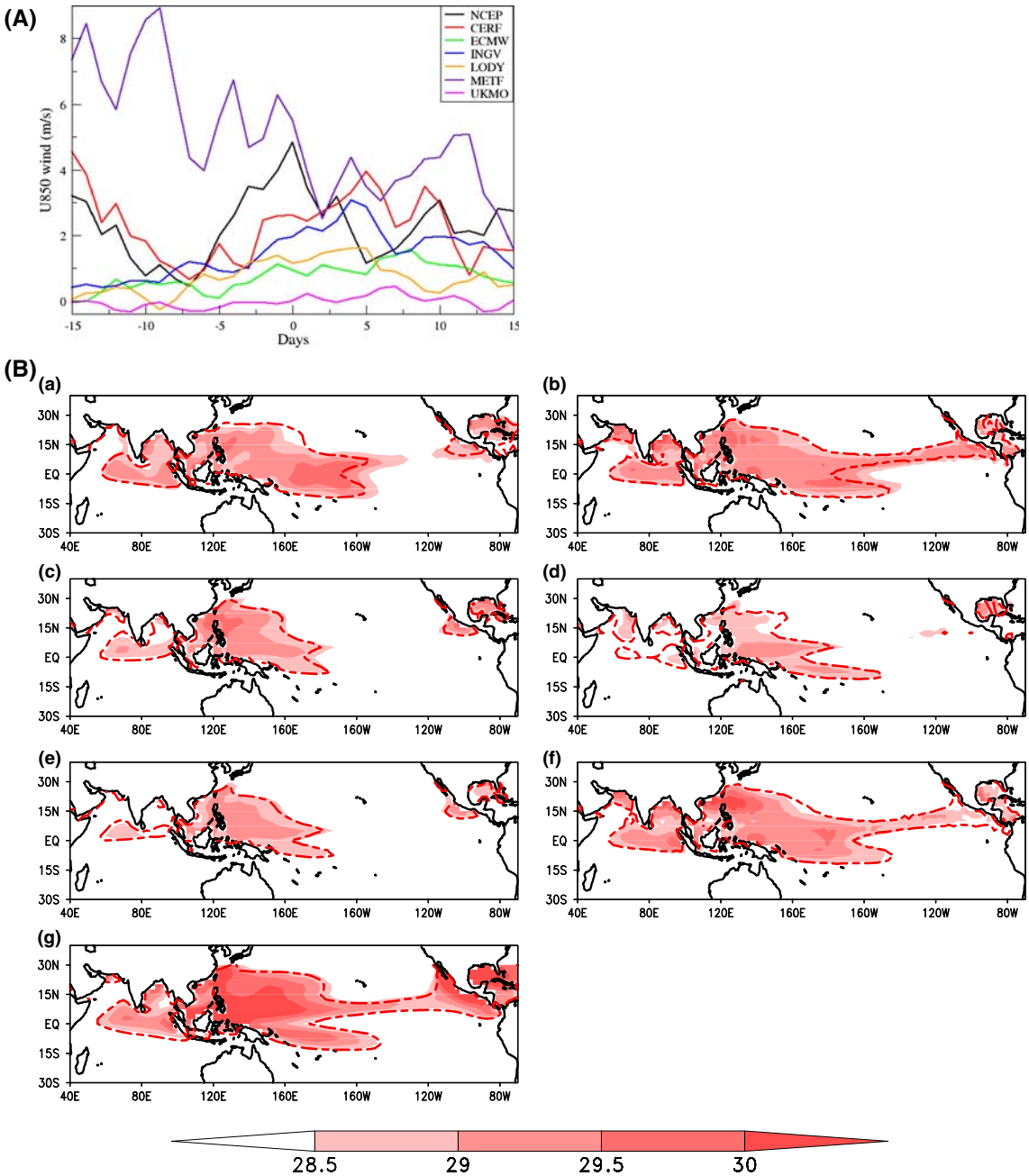


**Fig. 12** VLB composite of (**A**) zonal wind anomalies in m/s averaged over 150°–170°E; 5°S–5°N for observation and models. Here, zeroth day is the starting day of VLBs (**B**) actual SST in degree Celsius for observation and models. The 28.5°C isotherm of JJAS mean SST is marked as *dashed line*. **a** OBS, **b** CERF, **c** ECMW, **d** INGV, **e** LODY, **f** METF, **g** UKMO

external components seem to dominate the internal components. Also, the models with same AGCM exhibit similar climatological ISV patterns, whereas the ones sharing same OGCM have very disparate structure. This shows the dominant role of atmospheric components of these CGCMs in determining the nature of ISV activity which is consistent with the findings of Xavier et al. (2008). The study also emphasizes the need for accurate representation of air–sea interaction processes on intraseasonal time scale in the models. Two important requirements for this are: a high resolution ocean model to be able to simulate equatorial wave dynamics and an atmospheric model that would simulate the net heat flux to the ocean ($Q_{net}$) on ISO time scale realistically. The later requirement is related to the models' ability to simulate tropical clouds and its ISO variability with fidelity. This would require appropriate improvement of parameterization schemes for cloud, radiation and boundary layer.

**Acknowledgments** Susmitha Joseph acknowledges the Council of Scientific and Industrial Research (CSIR), Government of India for financial support. We also thank INDO-FRENCH project (Project No. 3907/1) for support and Dr. Prince K. Xavier of LMD/CNRS and Peter McLean of UK Met Office for making available the SST datasets from DEMETER project. We are also thankful to the two anonymous reviewers for their valuable, in-depth and constructive comments, which helped considerably in improving the scientific content of the present study. IITM is funded by Ministry of Earth Sciences (MoES), Government of India.

## References

Ajayamohan RS, Rao SA, Yamagata T (2008) Influence of Indian Ocean Dipole on poleward propagation of boreal summer intraseasonal oscillations. J Clim 21:5437–5454

Annamalai H, Slingo J (2001) Active/break cycles: diagnosis of the intraseasonal variability over the Asian summer monsoon. Clim Dyn 18:85–102

Ashok K, Guan Z, Yamagata T (2001) Impact of the Indian Ocean Dipole on the relationship between the Indian Monsoon Rainfall and ENSO. Geophys Res Lett 28:4499–4502. doi:10.1029/2001GL013294

Ashok K, Guan Z, Saji NH, Yamagata T (2004) Individual and combined influences of ENSO and the Indian Ocean Dipole on the Indian summer monsoon. J Clim 17:3141–3155

Ashok K, Behera SK, Rao SA, Weng H, Yamagata T (2007) El Nino Modoki and its possible teleconnection. J Geophys Res 112. doi:10.1029/2006JC003798

Bamzai AS, Shukla J (1999) Relation between Eurasian snow cover, snow depth, and the Indian summer monsoon: an observational study. J Clim 12:3117–3132

Bhalme HN, Jadhav SK, Mooley DA, Ramana Murty BhV (1986) Forecasting of monsoon performance over India. J Climatol 6:347–354

Blanford HF (1884) On the connection of the Himalaya snowfall with dry winds and seasons of drought in India. Proc R Soc Lond 37:3–22

Duchon CE (1979) Lanczos filtering in one and two dimensions. J Appl Meteorol 18:1016–1022

Ferranti L, Slingo JM, Palmer TN, Hoskins BJ (1997) Relations between interannual and intraseasonal monsoon variability as diagnosed from AMIP integrations. Quart J R Meteorol Soc 123:1323–1357

Gadgil S, Sajani S (1998) Monsoon precipitation in the AMIP runs. Clim Dyn 14:659–689

Gadgil S, Joseph PV, Joshi NV (1984) Ocean-atmosphere coupling over the monsoon regions. Nature 312:141–143

Goswami BN (1998) Interannual variation of Indian summer monsoon in a GCM: external conditions versus internal feedbacks. J Clim 11:501–522

Goswami BN (2005) South Asian Monsoon. In: Lau WKM, Waliser DE (eds) Intraseasonal variability in the atmosphere-ocean climate system, chap. 2, pp 19–61

Goswami BN, AjayaMohan RS (2001) Intraseasonal oscillations and interannual variability of the Indian summer monsoon. J Clim 14:1180–1198

Goswami P, Srividya (1996) A novel neural network design for long-range prediction of rainfall pattern. Curr Sci 70:447–457

Goswami BN, Xavier PK (2005) Dynamics of 'Internal' interannual variability of Indian Summer Monsoon in a GCM. J Geophys Res 110:D24104. doi:10.1029/2005JD006042

Goswami BN, Wu G, Yasunari T (2006) The annual cycle, intraseasonal oscillations and roadblock to seasonal predictability of the Asian summer monsoon. J Clim 19:5078–5099

Gowarikar V, Thapliyal V, Sarker RP, Mandal GS, Sikka DR (1989) Parametric and power regression models: new approach to long range forecasting of monsoon rain in India. Mausam 40:125–130

Gowarikar V, Thapliyal V, Kulshrestha SM, Mandal GS, Sen Roy N, Sikka DR (1991) A power regression model for long-range forecast of southwest monsoon rainfall over India. Mausam 42:125–130

Hoyos CD, Webster PJ (2007) The role of intraseasonal variability in the nature of Asian monsoon precipitation. J Clim 20:4402–4424

Jiang X, Li T, Wang B (2004) Structures and mechanisms of the northward propagating boreal summer intraseasonal oscillation. J Clim 17:1022–1039

Joseph S, Sahai AK, Goswami BN (2008) Eastward propagating MJO during boreal summer and Indian monsoon droughts. Clim Dyn. doi:10.1007/s00382-008-0412-8

Kang I-S, Shukla J (2006) Dynamic seasonal prediction and predictability of monsoon. In: Wang B (ed) The Asian monsoon, chap. 15, pp 585–612

Kang I-S, Jin K, Wang B, Lau K-M, Shukla J, Krishnamurthy V, Schubert S, Wailser DE, Stern W, Kitoh A, Meehl G, Kanamitsu M, Galin V, Satyan V, Park C-K, Liu Y (2002) Intercomparison of the climatological variations of Asian summer monsoon precipitation simulated by 10 GCMs. Clim Dyn 19:383–395

Kang I-S, Lee J-Y, Park C-K (2004) Potential predictability of summer mean precipitation in a dynamical seasonal prediction system with systematic error correction. J Clim 17:834–844

Kim H-M, Kang I-S, Wang B, Lee J-Y (2008) Interannual variations of the boreal summer intraseasonal variability predicted by ten atmosphere-ocean coupled models. Clim Dyn 30:485–496

Krishnan R, Zhang C, Sugi M (2000) Dynamics of breaks in the Indian summer monsoon. J Atmos Sci 57:1354–1372

Krishnan R, Kumar V, Sugi M, Yoshimura J (2009) Internal feedbacks from monsoon–midlatitude interactions during droughts in the Indian Summer Monsoon. J Atmos Sci 66:553–578

Madden RA, Julian PR (1971) Detection of a 40–50 day oscillation in the zonal wind in the tropical Pacific. J Atmos Sci 28:702–708

Madden RA, Julian PR (1994) Observations of the 40–50-day tropical oscillations—a review. Mon Weather Rev 122:814–837

Martin G, Dearden C, Greeves C, Hinton T, Inness P, James P, Pope V, Ringer M, Slingo J, Stratton R, Yang G-Y (2004) Evaluation of the atmospheric performance of HadGAM/GEM1. Hadley Centre Tech Note 54:1–64

Palmer TN, Alessandri A, Anderson U, Cantelaube P, Davey M, Délécluse P, Déqué M, Díez E, Dobblas-Reyers FJ, Fedderson H, Graham R, Gualdi S, Guérémy J-F, Hagedorn R, Hoshen M, Keenlyside N, Latif M, Lazar A, Maisonnave E, Marletto V, Morse AP, Orfila B, Rogel P, Terres J-M, Thomson MC (2004) Development of a European multimodel ensemble system for seasonal-to-interannual prediction (DEMETER). Bull Am Meteorol Soc 85:853–872

Rajeevan M, Pai DS, Thapliyal V (1998) Spatial and temporal relationships between global and surface air temperature anomalies and Indian summer monsoon. Meteorol Atmos Phys 66:157–171

Rajeevan M, Bhate J, Kale JD, Lal B (2006) High resolution daily gridded rainfall data for the Indian region: analysis of break and active monsoon spells. Curr Sci 91:296–306

Rajeevan M, Pai DS, Anil Kumar R, Lal B (2007) New statistical models for long-range forecasting of southwest monsoon rainfall over India. Clim Dyn 28:813–828

Rassmusson EM, Carpenter TH (1983) The relationship between eastern equatorial Pacific sea surface temperatures and rainfall over India and Srilanka. Mon Weather Rev 111:517–528

Reynolds RW, Smith TM (1994) Improved global sea surface temperature analyses using optimum interpolation. J Clim 7:929–948

Sahai AK, Soman MK, Satyan V (2000) All India summer monsoon rainfall prediction using artificial neural network. Clim Dyn 16:291–302

Sahai AK, Grimm AM, Satyan V, Pant GB (2002) Prospects of prediction of Indian summer monsoon rainfall using global SST anomalies. IITM Res Rep RR-093:1–44

Sahai AK, Grimm AM, Satyan V, Pant GB (2003) Long-lead prediction of Indian summer monsoon rainfall from Global SST evolution. Clim Dyn 20:855–863

Sahai AK, Chattopadhyay R, Goswami BN (2008) A SST based large multi-model ensemble forecasting system for Indian summer monsoon rainfall. Geophys Res Lett. doi: 10.1029/2008GL035461

Saji NH, Goswami BN, Vinayachandran PN, Yamagata T (1999) A dipole mode in the tropical Indian Ocean. Nature 401:360–363

Shukla J, Mooley DA (1987) Empirical prediction of the summer monsoon rainfall over India. Mon Weather Rev 115:695–704

Slingo JM, Sperber KR, Boyle JS, Ceron JP, Dix M, Dugas B, Ebisuzaki W, Fyfe J, Gregory D, Gueremy JF, Hack J, Harzallah A, Inness P, Kitoh A, Lau WKM, McAvaney B, Madden R, Mattews A, Palmer TN, Park CK, Randall D, Renno N (1996) Intraseasonal oscillations in 15 atmospheric general circulation models: results from an AMIP diagnostic subproject. Clim Dyn 12:325–357

Sperber KR, Palmer TN (1996) Interannual tropical rainfall variability in general circulation model simulations associated with Atmospheric Model Intercomparison Project. J Clim 9:2727–2750

Sperber KR, Brankovic C, Deque M, Frederiksen CS, Graham R, Kitoh A, Kobayashi C, Palmer TN, Puri K, Tennant W, Volodin E (2001) Dynamical seasonal predictability of the Asian summer monsoon. Mon Weather Rev 129:2226–2248

Taylor KE (2001) Summarizing multiple aspects of model performance in a single diagram. J Geophys Res 106(D7):7183–7192

Waliser DE, Jin K, Kang I-s, Stern SD, Schubert SD, Wu MC, Lau K-M, Lee M-I, Krishnamurthy V, Kitoh A, Meehl GA, Galin VY, Satyan V, Mandke SK, Wu G, Liu Y, Park C-K (2003) AGCM simulations of intraseasonal variability associated with the Asian summer monsoon. Clim Dyn 21:423–446

Walker GT (1923) Correlation in seasonal variations of weather. III: A preliminary study of world weather. Mem Ind Meteorol Dept 24:75–131

Walker GT (1924) Correlation in seasonal variations of weather. IV: A further study of world weather. Mem Ind Meteorol Dept 24:275–332

Walker GT, Bliss EW (1932) World weather. Mem R Meteorol Soc 4:53–84

Wang B, Kang I-S, Lee J-Y (2004) Ensemble simulations of Asian–Australian monsoon variability by 11 AGCMs. J Clim 17:699–710

Wang B, Ding QH, Fu XH, Kang I-S, Jin K, Shukla J, Doblas-Reyes F (2005) Fundamental challenge in simulation and prediction of summer monsoon rainfall. Geophys Res Lett 32:L15711

Wheeler M, Kiladis GN (1999) Convectively coupled equatorial waves: analysis of clouds and temperature in the wavenumber-frequency domain. J Atmos Sci 56:374–399

Xavier PK, Goswami BN (2007) A promising alternative to prediction of seasonal mean all India rainfall. Curr Sci 93:195–202

Xavier PK, Duvel JP, Doblas-Reyes FJ (2008) Boreal summer intraseasonal variability in coupled seasonal hindcasts. J Clim 21:4477–4497

Xie P, Arkin PA (1997) Global precipitation: a 17-year monthly analysis based on gauge observations, satellite estimates, and numerical model outputs. Bull Am Meteorol Soc 78:2539–2558

Xie P, Janowiak JE, Arkin PA, Adler RF, Gruber A, Ferraro RR, Huffman GJ, Curtis S (2003) GPCP Pentad precipitation analyses: an experimental dataset based on gauge observations and satellite estimates. J Clim 16:2197–2214